Eur. Phys. J. D **18**, 277–293 (2002)
DOI: 10.1140/epjd/e20020032

THE EUROPEAN PHYSICAL JOURNAL D
EDP Sciences

Properties of doubly excited states of H^- and He associated with the manifolds from N = 6 up to N = 25

S.I. Themelis[1,a], Y. Komninos[1,b], and C.A. Nicolaides[1,2,c]

[1] Theoretical and Physical Chemistry Institute, National Hellenic Research Foundation, 48 Vassileos Constantinou Ave., Athens 11635, Greece
[2] Physics Department, National Technical University, Athens, Greece

Received 10 September 2001 and Received in final form 12 November 2001

Abstract. This paper discusses theory and results on $^1P^0$ doubly excited states (DES) in He and in H^- of very high excitation, up to the $N = 25$ manifold. Our calculations employed full configuration interaction (CI) with large hydrogenic basis sets and produced correlated wavefunctions for the four lowest roots at each hydrogenic manifold by excluding open channels and the small contribution of series belonging to lower thresholds. The suitability of the hydrogenic basis sets for such calculations is justified, apart from their practicality, by the fact that, by computing from them natural orbitals, the results were shown to be the same with those of earlier multiconfigurational Hartree-Fock (MCHF) calculations on low-lying DES. In total, 160 states were computed, most of them for the first time. Their energy spectrum should be of use to possible future photoabsorption experiments. For certain low-lying DES up to $N = 13$, for which previous reliable results are available, comparison of the calculated energies shows good agreement. The correlated wavefunctions contain systematically chosen single and double excitations from each hydrogenic manifold of interest. From their analysis, we determined the "goodness" of different quantum numbers and the geometry (average angles and radii) as a function of excitation. For the Sinanoğlu-Herrick (K, T) classification scheme, whose basis is a restricted CI with hydrogenic functions and which has thus far been tested only on low-lying DES, we established that, whereas T remains a good index as energy increases, K does not. Consequently, a more flexible than K quantum number is needed in order to account for most of the additional correlation. This number, represented by $F = N - K - 1$, where N and K are *not* good numbers anymore, produces consistently a much higher degree of purity than the (K, T) scheme does, especially as N increases and as the relative significance of various virtual excitations due to electron correlation increases. Among the four states of each manifold, in all cases in H^- and in most cases in He, the three are of the intrashell type and one is of the intershell type with $(F, T) = (0, 0)$. The lowest intrashell states and the lowest intershell states exhibit a wide angle geometry tending to 180° as $N \to \infty$.

PACS. 31.25.Jf Electron correlation calculations for atoms and ions: excited states – 31.50.Df Potential energy surfaces for excited electronic states – 31.15.Ar Ab initio calculations – 32.80.Dz Autoionization

1 High-lying doubly excited states

Within the single configuration approximation of the shell model, the excitation of two electrons of an atom into the localized part, Ψ_0, of a doubly excited state (DES) with or without a core, can be represented by a wavefunction, which is a superposition of bound configurations. As with every electronic structure calculation, the rate of convergence to the solution of the Schrödinger equation depends on the combined choices of the type of the radial parts of the orbitals, and of the type and number of the two-electron configurations (in the field of the core – if present). The length and complexity of this superposition, which is the result of electron correlation (EC), increase rapidly with excitation energy because of a variety of near-degeneracies.

The excitation energy to which we refer here is the one that involves the excitation of both electrons, as the energy of the DES approaches the two-electron ionization threshold (TEIT), and not that involving only one electron as it is excited toward the one-electron ionization (detachment) threshold of a particular channel. A good index for marking the gross magnitude of this type of excitation is the value of the smaller of the two hydrogenic principal quantum numbers characterizing the zero order description. It is denoted by N. With respect to each N, we can divide the zero order configurations into intrashell, $(Nl_1,\ n_2l_2)$, if $N = n_1 = n_2$, into intershell, $(Nl_1,\ n_2l_2)$,

[a] e-mail: stheme@eie.gr
[b] e-mail: ykomn@eie.gr
[c] e-mail: can@eie.gr

if $n_1 = N < n_2$, and into doubly excited, $(n_1' l_1,\ n_2' l_2)$, if $n_1' > n_1$ and $n_2' > n_2$. Each localized correlated wavefunction of a DES is a superposition of these configurations for all values of the hydrogenic numbers prescribed by the theory. We write the corresponding wavefunction as Ψ_v.

The large variety of mixing configurations leads to a multitude of possible valid solutions Ψ_v representing DES. In principle, the results of this large number of possible superpositions are complex spectral features. It is reasonable to expect that theoretical efforts should aim at extracting certain *regularities* of the energy spectrum and of other properties out of this complexity. The present theory and calculations constitute a contribution to this purpose.

As already stated, the length and complexity of each such superposition increases rapidly with N. It is for this reason that the available data are from computations for *low* N, where "low" is qualified below. These data have already led to certain conclusions about regularities, as N increases, in the wavefunctions, energies and widths of a class of states of DES consisting of the states of lowest energy at each manifold N [1–4]. However, in order to truly establish these regularities in a quantitative way and to provide additional understanding in the continuing exploration of electron correlations in such states, it is desirable to investigate parts of the spectrum for larger values of N, where much more complex situations of possible mixings of configurations and of perturbed spectra ought to exist. Furthermore, in doing so, it is also desirable to calculate not only the lowest energy state of each intrashell manifold, but a few of them, in order to obtain information on the properties of groups of such states and on their behaviour with increasing N, as they reach the infinitely degenerate $E = 0$ state.

Such a desideratum has made matters for experimental and theoretical spectroscopy rather difficult, even in the simplest of atoms, H^- and He, as soon as N reaches values around 10–15. It is then natural to ask the question of how to solve the problem of the determination and interpretation of accurate wavefunctions and of the concomitant properties for values of N higher than 10–15. It is this question that has led some researchers on the one hand to express rather pessimistic remarks about the treatment of electron correlation in DES by configuration-interaction (CI)-type methods and on the other hand to argue in favor of formalisms based on collective coordinates (without this meaning that such calculations have indeed been achieved) (*e.g.*, [5–10]). For example, Zhang and Rau ([6], p. 6934), before presenting their electron-pair analysis for obtaining information on the *ridge states*, write: "*Strong two-electron correlations lead to large mixings and, given the diverging number of Coulomb states with increasing excitation, these calculations, (close-coupling method or configuration interaction), become impractical for the high doubly excited states*".

It is not clear from [6] to which level of excitation "*high doubly excited state*" refers. Here, in a somewhat arbitrary fashion, which, however, has to do with the existing literature on DES, (to the best of our knowledge), and with changes in the level of difficulty of computation, we will refer to *DES of H^- and He with $N \leq 15$ as low-lying and those above as high-lying*. The present results pertain to both regimes.

Even for low-lying DES, only a few calculations have reached the excitation energies between $N = 10$ and $N = 15$ [1–4,6–10]. For example, using the method of *hyperspherical coordinates in the adiabatic approximation*, Sadeghpour [7] calculated the energies of $^1P^0$ DES of He up to $n = 10$ and of H^- up to $n = 12$. Rost and Briggs [10] implemented their *adiabatic molecular orbital* theory and obtained energies for He and H^- DES of ^1S and $^1P^0$ symmetries up to $n = 10$–13. Komninos *et al.* [3], published in a preliminary report the essential results of CI calculations on DES of H^-, He and Li^+ for ^1S and $^1P^0$ symmetries, obtained from fully correlated wavefunctions with one- and two-electron excitations at each manifold, up to $N = 15$. These wavefunctions were then used to analyze properties of these states. This is the approach that we have followed in this work, where we have determined the correlated wavefunctions and various properties of the lowest four DES at each manifold, up to $N = 25$.

One of the basic reasons for the lack of reliable data on DES of the high regime is the associated computational complexity and the associated difficulty in developing and applying an appropriate theoretical approach. Yet, this part of the spectrum of DES is one of the intriguing frontiers of atomic spectroscopy, which have remained outside the reach of experiment and which can serve as grounds for the continuing testing of the methods of computation of atomic structure, of electron correlation and of properties in excited states. Now, apart from the enormous size of hydrogenic degeneracies at each N manifold, there is entanglement of the N manifolds with channels represented by $n_2 > n_1$ configurations, as well as increasing proximity among the N manifolds themselves. Therefore, the problem has to be understood reasonably well, theoretically as well as numerically, so that it can be formulated and solved in a practical way. Another reason for the importance of the high regime is because, in principle, accurate wavefunction and spectral information can be used as reference for the evaluation of semiclassical calculations and interpretations (*e.g.*, [11–13]).

The work whose results we present here has dealt with low- as well as high-lying N-manifold DES of $^1P^0$ symmetry, (an experimentally reachable symmetry from the ground state), in H^- and He, up to $N = 25$. In total, 160 states were computed, most of them for the first time. Numerical results for all of them are reported − rather than for selected few − since we think that all of them and each one individually may prove useful to future theoretical and experimental investigations.

The calculations were of the CI-type. They were managed successfully by utilizing our earlier experience with basis functions and magnitudes of interaction matrix elements, by improving the numerical techniques and by taking advantage of the availability of the necessary computer power. The value of $N = 25$ was deemed sufficient for allowing substantial analysis and for drawing generally valid conclusions about the feasibility of computing *ab initio*

DES of very high N and about the properties of the lowest few intrashell states of each manifold. These properties include their energies, their geometries, their wavefunction CI characteristics and their labeling by "*quasi-good*" quantum numbers. The corresponding levels of excitation are 0.029 eV below the TEIT of H^-, which is at 14.3530 eV, (1 a.u. (H^-) = 27.1966 eV), and 0.143 eV below that of He, which is at 79.004 eV (1 a.u. (He) = 27.2077 eV). The choice of the two atomic species, H^- and He, was based on the known facts about the differences in the strength and type of their potentials and in the relative significance of electron correlation, which changes considerably from $Z = 2$ to $Z = 1$.

2 Brief review of results on doubly excited states relevant to this work

The focus of this work was the class of DES that can be identified as *intrashell* states for each manifold defined by N. As we shall recall below, the lowest state for each N is always of the intrashell type with special properties. Having understood how to compute them systematically, in this work we applied practical methods for the calculation and analysis of DES which correspond not only to the lowest energy of their symmetry at each manifold N but to the first few, (four in this case), energies. Apart from energies, we aimed at determining possible regularities in their character and in their geometrical features.

Aspects of the background to such calculations are summarized below.

Fano's review [5] on the "*correlations of two excited electrons*" reported on advances that had occurred over the previous twenty years. Special attention was given to descriptions in terms of collective coordinates and to the related elementary phenomenology of intrashell DES possibly connected to the physics of the two-electron ionization at threshold. At that time, the quantum mechanical analysis of the wavefunctions and properties of DES as they change with N, lacked quantitative support. Therefore, discussions on the "*Wannier ridge states*", the properties of which are also discussed in the present paper, did not include quantitative predictions of measurable properties and were by necessity based on scarce semiquantitative data and on hypothesis.

The first systematic quantum mechanical calculations and analysis of the properties of intrashell DES of $^1P^0$ symmetry in H^-, He and Li^+ along the N manifolds, (up to $N = 10$), were presented a few years after Fano's review [1,2,14]. They were based on CI-type schemes and produced reliable information and conclusions which have been of use in subsequent work. For example, Komninos and Nicolaides [1,2] published energies, wavefunction characteristics, geometrical properties and absorption oscillator strengths up to $N = 10$, for the lowest energy intrashell state at each N manifold. Robaux [14] provided an analysis of DES wavefunctions for He up to $N = 6$ in terms of the (K, T) scheme of Sinanoğlu and Herrick [15,16] and discussed aspects of the properties of Rydberg series of "*ridge states*" and of the interaction between states belonging to different N manifolds. Calculation of the $^1P^0$ DES and of properties along the N manifolds were later also produced by the application of methods using collective coordinates [6–10].

One of the aims of the work that led to [1,2] was to demonstrate the possibility of computing correlated wavefunctions for various manifolds N, (at the time, $N = 10$ was numerically possible and sufficient for the purposes), in terms of suitably chosen zero order and correlation configurations, consisting of numerical self-consistent orbitals and of analytic virtual orbitals. As a result, it became possible to identify eigenfunctions, which have certain *regular properties as excitation increases toward the TEIT*. These states were named the Wannier *two-electron ionization ladder* (TEIL) states [1,2]. Their existence had been hypothesized in the early 1980's as the natural extension below the TEIT of the Wannier classical state at $E = 0$, with related descriptions in terms of hyperspherical coordinates (hsc) [5,17,18]. They were named *Wannier ridge* states, where the Wannier ridge is defined classically by $r_1 = r_2$ and $\theta_{12} = \pi$. Given this classically conceived special class of DES, arguments about the stability of these states were advanced, without quantum mechanical computation of their decay widths. For example, Rau [17], in his discussion of the spectrum of the He^- ^2S resonances measured by Buckman *et al.* [18], concludes: "*...This makes the access to these states difficult and conversely, once accessed, makes for their long stability*". However, if we take from the literature of DES accurate results on widths and isolate those of lowest energy at each N-manifold, we see that, in fact, the *Wannier ridge states* have no distinct and/or systematic stability toward autoionization as compared with other DES. This is evident from quantum mechanical results on H^- and He as well as on He^-. For example, a look at Table 1 of [19], exhibiting the widths of He^- ^4P DES, shows that, of the computed DES associated with each He $1snp$ $^3P^0$ threshold, the lowest energy state is the least stable. On the other hand, the stability toward autoionization of each such state increases with N [4,19].

The application of CI-type methods with judiciously chosen and optimized function spaces, has revealed physically relevant properties of the TEIL states quantum mechanically, [1–4] and references therein. Apart from the energies and the demonstration of their regularity with N, a fact which allows reasonably accurate extrapolations to very high N based on spectral formulae, critical information about wavefunction characteristics and partial widths has been obtained. For example, it was found quantitatively how the main configurational constitution of each TEIL state changes as N increases. This feature was computed for a number of symmetries. For the $^1P^0$ symmetry which is of interest here, it was determined that for He, although for the TEIL state of $N = 3$ the $(3s3p)$ configuration dominates, starting already at $N = 4$ the $(4p4d)$ configuration dominates, while at $N = 10$ the $(10d10f)$ configuration takes over, with a coefficient 0.6014 ([2], Tab. 3). It follows that discussions about such series of

Table 1. He $^1P^0$ doubly excited states up to $N = 25$, according to the approach of this paper. The four lowest localized solutions at each manifold N were obtained. The majority of these states were computed in this work for the first time. Labels, energies, angles and degree of purity of states in the Herrick-Sinanoğlu (K, T) scheme and in the (F, T) scheme are given. The lowest one at each N is a Wannier TEIL state. For the $T = 1$ states, the higher ones have smaller angles for all N, reflecting the progressive reduction of electron correlation effects.

		$N(F,T)_n^A$	E (a.u.)	$\langle\theta_{12}\rangle$	$P(KT)$	$P(FT)$
$N = 6$	$^1P^0(1)$	$6\ (1,1)_6^+$	−0.089021	130.2	0.997	0.997
	$^1P^0(2)$	$6\ (3,1)_6^+$	−0.085019	112.1	0.981	0.983
	$^1P^0(3)$	$6\ (5,1)_6^+$	−0.079875	99.0	0.919	0.928
	$^1P^0(4)$	$6\ (0,0)_7^-$	−0.079599	147.0	0.997	0.999
$N = 7$	$^1P^0(1)$	$7\ (1,1)_7^+$	−0.065903	134.4	0.997	0.998
	$^1P^0(2)$	$7\ (3,1)_7^+$	−0.063569	117.6	0.984	0.986
	$^1P^0(3)$	$7\ (5,1)_7^+$	−0.060682	105.4	0.935	0.943
	$^1P^0(4)$	$7\ (0,0)_8^-$	−0.059602	149.7	0.997	0.999
$N = 8$	$^1P^0(1)$	$8\ (1,1)_8^+$	−0.050743	137.7	0.997	0.998
	$^1P^0(2)$	$8\ (3,1)_8^+$	−0.049271	122.1	0.984	0.987
	$^1P^0(3)$	$8\ (5,1)_8^+$	−0.047501	110.6	0.943	0.951
	$^1P^0(4)$	$8\ (0,0)_9^-$	−0.046322	151.8	0.996	0.999
$N = 9$	$^1P^0(1)$	$9\ (1,1)_9^+$	−0.040271	140.4	0.997	0.998
	$^1P^0(2)$	$9\ (3,1)_9^+$	−0.039286	125.8	0.984	0.987
	$^1P^0(3)$	$9\ (5,1)_9^+$	−0.038129	114.9	0.947	0.955
	$^1P^0(4)$	$9\ (0,0)_{10}^-$	−0.037047	153.6	0.995	0.999
$N = 10$	$^1P^0(1)$	$10\ (1,1)_{10}^+$	−0.032737	142.8	0.996	0.998
	$^1P^0(2)$	$10\ (3,1)_{10}^+$	−0.032048	129.0	0.983	0.987
	$^1P^0(3)$	$10\ (5,1)_{10}^+$	−0.031252	118.5	0.948	0.956
	$^1P^0(4)$	$10\ (7,1)_{10}^+$	−0.030330	110.3	0.872	0.885
$N = 11$	$^1P^0(1)$	$11\ (1,1)_{11}^+$	−0.027136	144.7	0.995	0.998
	$^1P^0(2)$	$11\ (3,1)_{11}^+$	−0.026636	131.7	0.982	0.987
	$^1P^0(3)$	$11\ (5,1)_{11}^+$	−0.026067	121.7	0.948	0.956
	$^1P^0(4)$	$11\ (7,1)_{11}^+$	−0.025417	113.8	0.877	0.890
$N = 12$	$^1P^0(1)$	$12\ (1,1)_{12}^+$	−0.022860	146.5	0.994	0.997
	$^1P^0(2)$	$12\ (3,1)_{12}^+$	−0.022486	134.0	0.980	0.986
	$^1P^0(3)$	$12\ (5,1)_{12}^+$	−0.022066	124.5	0.946	0.955
	$^1P^0(4)$	$12\ (7,1)_{12}^+$	−0.021592	116.9	0.879	0.892
$N = 13$	$^1P^0(1)$	$13\ (1,1)_{13}^+$	−0.019522	148.0	0.993	0.997
	$^1P^0(2)$	$13\ (3,1)_{13}^+$	−0.019235	136.1	0.978	0.985
	$^1P^0(3)$	$13\ (5,1)_{13}^+$	−0.018916	127.0	0.943	0.954
	$^1P^0(4)$	$13\ (7,1)_{13}^+$	−0.018560	119.6	0.878	0.892
$N = 14$	$^1P^0(1)$	$14\ (1,1)_{14}^+$	−0.016865	149.3	0.992	0.997
	$^1P^0(2)$	$14\ (3,1)_{14}^+$	−0.016641	137.9	0.976	0.983
	$^1P^0(3)$	$14\ (5,1)_{14}^+$	−0.016394	129.2	0.940	0.951
	$^1P^0(4)$	$14\ (7,1)_{14}^+$	−0.016120	122.0	0.875	0.890
$N = 15$	$^1P^0(1)$	$15\ (1,1)_{15}^+$	−0.014717	150.6	0.990	0.996
	$^1P^0(2)$	$15\ (3,1)_{15}^+$	−0.014539	139.6	0.973	0.982
	$^1P^0(3)$	$15\ (5,1)_{15}^+$	−0.014343	131.2	0.936	0.949
	$^1P^0(4)$	$15\ (7,1)_{15}^+$	−0.014129	124.2	0.871	0.887
$N = 16$	$^1P^0(1)$	$16\ (1,1)_{16}^+$	−0.012955	151.6	0.988	0.996
	$^1P^0(2)$	$16\ (3,1)_{16}^+$	−0.012811	141.1	0.970	0.980
	$^1P^0(3)$	$16\ (5,1)_{16}^+$	−0.012654	132.9	0.932	0.946
	$^1P^0(4)$	$16\ (7,1)_{16}^+$	−0.012483	126.2	0.866	0.883

Table 1. *Continued.*

		$N(F,T)_n^A$	E (a.u.)	$\langle\theta_{12}\rangle$	$P(KT)$	$P(FT)$
$N=17$	$^1P^0(1)$	17 $(1,1)^+_{17}$	−0.011492	152.6	0.987	0.995
	$^1P^0(2)$	17 $(3,1)^+_{17}$	−0.011374	142.4	0.967	0.979
	$^1P^0(3)$	17 $(5,1)^+_{17}$	−0.011246	134.6	0.927	0.942
	$^1P^0(4)$	17 $(7,1)^+_{17}$	−0.011107	128.0	0.861	0.879
$N=18$	$^1P^0(1)$	18 $(1,1)^+_{18}$	−0.010264	153.5	0.985	0.995
	$^1P^0(2)$	18 $(3,1)^+_{18}$	−0.010166	143.7	0.963	0.977
	$^1P^0(3)$	18 $(5,1)^+_{18}$	−0.010061	136.0	0.922	0.939
	$^1P^0(4)$	18 $(7,1)^+_{18}$	−0.009947	129.7	0.854	0.874
$N=19$	$^1P^0(1)$	19 $(1,1)^+_{19}$	−0.009223	154.4	0.983	0.994
	$^1P^0(2)$	19 $(3,1)^+_{19}$	−0.009141	144.8	0.960	0.975
	$^1P^0(3)$	19 $(5,1)^+_{19}$	−0.009053	137.4	0.917	0.935
	$^1P^0(4)$	19 $(7,1)^+_{19}$	−0.008958	131.2	0.848	0.868
$N=20$	$^1P^0(1)$	20 $(1,1)^+_{20}$	−0.008333	155.1	0.980	0.994
	$^1P^0(2)$	20 $(3,1)^+_{20}$	−0.008264	145.9	0.956	0.973
	$^1P^0(3)$	20 $(5,1)^+_{20}$	−0.008189	138.7	0.911	0.931
	$^1P^0(4)$	20 $(7,1)^+_{20}$	−0.008110	132.7	0.841	0.863
$N=21$	$^1P^0(1)$	21 $(1,1)^+_{21}$	−0.007566	155.8	0.978	0.993
	$^1P^0(2)$	21 $(3,1)^+_{21}$	−0.007507	146.8	0.952	0.971
	$^1P^0(3)$	21 $(5,1)^+_{21}$	−0.007444	139.8	0.906	0.927
	$^1P^0(4)$	21 $(7,1)^+_{21}$	−0.007377	134.0	0.834	0.857
$N=22$	$^1P^0(1)$	22 $(1,1)^+_{22}$	−0.006900	156.5	0.976	0.993
	$^1P^0(2)$	22 $(3,1)^+_{22}$	−0.006850	147.7	0.949	0.969
	$^1P^0(3)$	22 $(5,1)^+_{22}$	−0.006796	140.9	0.900	0.923
	$^1P^0(4)$	22 $(7,1)^+_{22}$	−0.006738	135.2	0.826	0.851
$N=23$	$^1P^0(1)$	23 $(1,1)^+_{23}$	−0.006319	157.1	0.973	0.992
	$^1P^0(2)$	23 $(3,1)^+_{23}$	−0.006275	148.5	0.945	0.967
	$^1P^0(3)$	23 $(5,1)^+_{23}$	−0.006229	141.9	0.894	0.920
	$^1P^0(4)$	23 $(7,1)^+_{23}$	−0.006179	136.3	0.819	0.845
$N=24$	$^1P^0(1)$	24 $(1,1)^+_{24}$	−0.005808	157.6	0.971	0.992
	$^1P^0(2)$	24 $(3,1)^+_{24}$	−0.005770	149.3	0.941	0.965
	$^1P^0(3)$	24 $(5,1)^+_{24}$	−0.005730	142.8	0.888	0.916
	$^1P^0(4)$	24 $(7,1)^+_{24}$	−0.005687	137.4	0.811	0.839
$N=25$	$^1P^0(1)$	25 $(1,1)^+_{25}$	−0.005357	158.2	0.968	0.991
	$^1P^0(2)$	25 $(3,1)^+_{25}$	−0.005324	150.1	0.937	0.964
	$^1P^0(3)$	25 $(5,1)^+_{25}$	−0.005288	143.7	0.883	0.912
	$^1P^0(4)$	25 $(7,1)^+_{25}$	−0.005251	138.4	0.803	0.833

states which have used only one configuration as a constant zero order label, (*e.g.* use of (core) Ns^2 for deducing semiempririca formulae for ^{1}S states), have an unjustifiable zero order reference point. In fact, for these states, the zero order description is by necessity multiconfigurational, with the mixing coefficients changing with N and leading to different dominant configurations already in the regime of low − lying DES.

Once fully correlated CI-type wavefunctions for DES have been calculated, appropriate computations can obtain information about geometry, classification, nodal structure and other properties, [1–4] and references therein. For example, conditional probability plots and conditional expectation values showed that the lowest energy intrashell state at each N manifold of the low-regime has the quantum mechanical property that $\langle r_1\rangle$ is close to $\langle r_2\rangle|_{r_1=\langle r_1\rangle}$ (see Eq. (10)). The relation $\langle r_1\rangle = \langle r_2\rangle|_{r_1=\langle r_1\rangle}$ is the analogue of the Wannier classical condition $r_1 = r_2$ at $E = 0$.

In Section 4, we present systematic results of $\langle r_1\rangle$ and $\langle r_2\rangle|_{r_1=\langle r_1\rangle}$ for the lowest four energy states at each N, up to $N = 25$.

Calculations were also done for θ_{12}, the angle between the two radius vectors, of the lowest energy intrashell state at each N in the low regime. It was found that this angle starts rather far from the Wannier ridge condition, $\theta_{12} = 180°$, and tends very slowly to 180° as $N \to \infty$, *i.e.* as the mixing of configurations increases. This is a result, which is predicted by the restricted-space model and analysis of Herrick, Kellman and Poliak [20,21] and which is further examined quantitatively in the present paper. It is significant to add here that similarly smooth and excitation-dependent geometrical properties were identified and analyzed by state-specific calculations on *hyper-ridge* ladders of triply [22] and quadruply [23] excited states leading to their corresponding fragmentation thresholds.

The theory of [1–4] employed state-specific configurations and well-optimized orbitals for the intrashell multiconfigurational (MC) zero order description and for the one- and two-electron correlation functions. The zero order orbitals are either MC Hartree-Fock (MCHF) or *natural orbitals*, the latter having been shown [3] to produce the same results while they are directly computable from hydrogenic CI. The approach based on zero order natural orbitals for the intrashell configurations was developed [3] in order to bypass the numerical bottlenecks, which exist when requiring the calculation of accurate state-specific numerical MCHF wavefunctions for N in the high regime. Once the zero order MCHF orbital space is available, the correlation orbitals are expressed in terms of Slater-type orbitals (STO), which are optimized during the minimization of the total energy subject to appropriate orthogonality conditions [1,2].

We point out that the structure of the state-specific approach to the quantitative understanding of the DES, and of multiply excited states in general, is such that polyelectronic atoms can be treated systematically. Specifically, the fact that at least in the low regime it is possible to obtain MCHF solutions, albeit with difficulty and after considerable experience, permits the calculation of DES where a closed or an open-shell electron core is present and is allowed to interact *self-consistently* with the valence electrons. Of course, as the manifold index N increases, the core-valence coupling decreases rapidly and the spectrum is dominated by the self-consistent correlated motion of just the pair of excited electrons [24].

The possibility of obtaining *ab initio* fully correlated wavefunctions of intrashell DES for each manifold N and of identifying the TEIL state as that with the lowest energy at each N, has also allowed the calculation of properties previously discussed in the context of either semiclassical frameworks or model quantum mechanical function spaces. Specifically, the quantum mechanical calculations of Nicolaides and Komninos [25] produced numbers for the N-dependence of the partial width to the ground state channel of the H^- TEIL states of ^1S symmetry, which could be compared with the formulae obtained earlier semiclassically. They found $\Gamma(N) \sim N^{-6.8\pm0.4}$, where the uncertainty was estimated from the possible errors in the overall calculation. More recent calculations by Heim and Rau [26], using hyperspherical coordinates, produced $\Gamma(N) \sim N^{-6.5}$.

The degree of "goodness" of new quantum numbers

Finally, another set of results contributing to the quantitative understanding of the N-dependence of properties of intrashell DES is to be found in the study of Komninos *et al.* [3] on the degree of goodness of the Sinanoğlu-Herrick [15,16] (K,T) scheme of labeling DES of two-electron atoms, and on the therein proposed (F,T) scheme, where F is a combination of N and K, neither of which is now a "*good*" quantum number. Specifically,

$$F = N - 1 - K \tag{1}$$

where K goes from $-N-1-T$ to $N-1-T$, in steps of 2.

As we pointed out in [3], F is numerically the same quantity as v, the number of bending quanta in the linear rotor-vibrator picture of DES introduced in [20,21]. (see also [27]). However, the connection stops here, since the combination of N and K in (1) is used in [20,21,27] only formally and descriptively, assuming that K and N are "*good*" numbers. In fact, it is the recognition that this combination expresses to a very good approximation the fully correlated wavefunctions of DES, contrary to the (K,T) scheme, that distinguishes the definition and quantitative use of v in [20,21,27] from that of F in [3] and in the present work. At the same time, the finding that F is a rather good number lends support to the molecular models of Herrick and Kelmann [20] and of Feagin, Rost and Briggs [10]. These authors have assumed an approximate decoupling of a transformed two-electron Hamiltonian, according to which v is a good number.

It was found in [3], and is confirmed in the present work, that even for the TEIL states, which are rather distinct from the other types of superpositions, the F,T classification gives "purer" vectors. For example, as shown in Table 2 of this paper, for the ($N = 25$, $n_2 = 25$) TEIL $^1P^0$ state in H^-, the purity for (K,T) is 0.845 whereas that for (F,T) is 0.975. This type of discrepancy is reduced as Z increases, ([3] and this work), because the origin of the (K,T) scheme lies with the O(4) group properties of the Coulomb potential and with the use of the restricted model space of only intrashell configurations with hydrogen orbitals, named the *doubly excited symmetry basis* (DESB) [15,16,21]. Therefore, even for the lowest energy state where the angular correlation dominates, the degree of deterioration of the goodness of N and K can be uncovered systematically by obtaining the full electron correlation for increasing values of N and decreasing binding to the nucleus. In this context, we stress that the correct and meaningful way of extracting the (K,T) content from well-correlated wavefunctions, is the projection onto the DESB. In some *ab initio* investigations of DES, this is indeed what has been done, [3,14,27]. However, in other works, (*e.g.*, [29,30]), this classification is done only by conjecture. In addition to lack of rigor, given the

Table 2. As in Table 1, for H^-. The intershell state, $T = 0$, remains as one of the four lowest states up to $N = 25$.

		$N(F,T)_n^A$	E (a.u.)	$\langle\theta_{12}\rangle$	$P(KT)$	$P(FT)$
$N = 6$	$^1P^0(1)$	$6\ (1,1)_6^+$	−0.017560	134.4	0.975	0.988
	$^1P^0(2)$	$6\ (0,0)_7^-$	−0.016150	149.3	0.983	0.996
	$^1P^0(3)$	$6\ (3,1)_6^+$	−0.016037	118.1	0.902	0.933
	$^1P^0(4)$	$6\ (1,1)_7^+$	−0.015307	134.6	0.930	0.986
$N = 7$	$^1P^0(1)$	$7\ (1,1)_7^+$	−0.013109	138.2	0.971	0.988
	$^1P^0(2)$	$7\ (3,1)_7^+$	−0.012202	123.2	0.904	0.937
	$^1P^0(3)$	$7\ (0,0)_8^-$	−0.012103	151.8	0.979	0.996
	$^1P^0(4)$	$7\ (1,1)_8^+$	−0.011529	138.3	0.902	0.985
$N = 8$	$^1P^0(1)$	$8\ (1,1)_8^+$	−0.010158	141.3	0.967	0.987
	$^1P^0(2)$	$8\ (3,1)_8^+$	−0.009578	127.3	0.902	0.939
	$^1P^0(3)$	$8\ (0,0)_9^-$	−0.009417	153.9	0.974	0.996
	$^1P^0(4)$	$8\ (1,1)_8^+$	−0.009013	141.2	0.868	0.979
$N = 9$	$^1P^0(1)$	$9\ (1,1)_9^+$	−0.008103	143.8	0.962	0.987
	$^1P^0(2)$	$9\ (3,1)_9^+$	−0.007711	130.7	0.898	0.938
	$^1P^0(3)$	$9\ (0,0)_{10}^-$	−0.007541	155.6	0.968	0.996
	$^1P^0(4)$	$9\ (5,1)_9^+$	−0.007263	120.9	0.776	0.828
$N = 10$	$^1P^0(1)$	$10\ (1,1)_{10}^+$	−0.006615	145.9	0.956	0.986
	$^1P^0(2)$	$10\ (3,1)_{10}^+$	−0.006338	133.5	0.892	0.937
	$^1P^0(3)$	$10\ (0,0)_{11}^-$	−0.006178	157.0	0.963	0.995
	$^1P^0(4)$	$10\ (5,1)_{10}^+$	−0.006025	124.2	0.779	0.834
$N = 11$	$^1P^0(1)$	$11\ (1,1)_{11}^+$	−0.005503	147.7	0.950	0.985
	$^1P^0(2)$	$11\ (3,1)_{11}^+$	−0.005300	136.0	0.886	0.935
	$^1P^0(3)$	$11\ (0,0)_{12}^-$	−0.005156	158.2	0.957	0.995
	$^1P^0(4)$	$11\ (5,1)_{11}^+$	−0.005074	127.1	0.776	0.834
$N = 12$	$^1P^0(1)$	$12\ (1,1)_{12}^+$	−0.004650	149.3	0.943	0.985
	$^1P^0(2)$	$12\ (3,1)_{12}^+$	−0.004498	138.1	0.878	0.933
	$^1P^0(3)$	$12\ (0,0)_{13}^-$	−0.004369	159.3	0.950	0.995
	$^1P^0(4)$	$12\ (5,1)_{12}^+$	−0.004329	129.5	0.770	0.832
$N = 13$	$^1P^0(1)$	$13\ (1,1)_{13}^+$	−0.003981	150.7	0.936	0.984
	$^1P^0(2)$	$13\ (3,1)_{13}^+$	−0.003864	139.9	0.871	0.930
	$^1P^0(3)$	$13\ (0,0)_{14}^-$	−0.003751	160.2	0.943	0.994
	$^1P^0(4)$	$13\ (5,1)_{13}^+$	−0.003735	131.7	0.763	0.829
$N = 14$	$^1P^0(1)$	$14\ (1,1)_{14}^+$	−0.003447	151.9	0.929	0.983
	$^1P^0(2)$	$14\ (3,1)_{14}^+$	−0.003355	141.6	0.862	0.928
	$^1P^0(3)$	$14\ (0,0)_{15}^-$	−0.003256	161.0	0.936	0.994
	$^1P^0(4)$	$14\ (5,1)_{14}^+$	−0.003255	133.7	0.756	0.826
$N = 15$	$^1P^0(1)$	$15\ (1,1)_{15}^+$	−0.003015	153.0	0.922	0.982
	$^1P^0(2)$	$15\ (3,1)_{15}^+$	−0.002941	143.1	0.854	0.925
	$^1P^0(3)$	$15\ (5,1)_{15}^+$	−0.002861	135.4	0.748	0.822
	$^1P^0(4)$	$15\ (0,0)_{16}^-$	−0.002853	161.7	0.929	0.993
$N = 16$	$^1P^0(1)$	$16\ (1,1)_{16}^+$	−0.002659	154.0	0.914	0.982
	$^1P^0(2)$	$16\ (3,1)_{16}^+$	−0.002599	144.4	0.846	0.923
	$^1P^0(3)$	$16\ (5,1)_{16}^+$	−0.002534	137.0	0.739	0.818
	$^1P^0(4)$	$16\ (0,0)_{17}^-$	−0.002521	162.4	0.922	0.993
$N = 17$	$^1P^0(1)$	$17\ (1,1)_{17}^+$	−0.002362	154.9	0.907	0.981
	$^1P^0(2)$	$17\ (3,1)_{17}^+$	−0.002313	145.6	0.837	0.920
	$^1P^0(3)$	$17\ (5,1)_{17}^+$	−0.002260	138.5	0.731	0.814
	$^1P^0(4)$	$17\ (0,0)_{18}^-$	−0.002244	163.0	0.914	0.993

Table 2. *Continued.*

		$N(F,T)_n^A$	E (a.u.)	$\langle\theta_{12}\rangle$	$P(KT)$	$P(FT)$
$N=18$	$^1P^0(1)$	18 $(1,1)^+_{18}$	−0.002113	155.7	0.899	0.980
	$^1P^0(2)$	18 $(3,1)^+_{18}$	−0.002072	146.7	0.829	0.918
	$^1P^0(3)$	18 $(5,1)^+_{18}$	−0.002028	139.8	0.722	0.809
	$^1P^0(4)$	18 $(0,0)^-_{19}$	−0.002011	163.5	0.907	0.992
$N=19$	$^1P^0(1)$	19 $(1,1)^+_{19}$	−0.001901	156.4	0.891	0.979
	$^1P^0(2)$	19 $(3,1)^+_{19}$	−0.001867	147.7	0.820	0.915
	$^1P^0(3)$	19 $(5,1)^+_{19}$	−0.001830	141.0	0.713	0.805
	$^1P^0(4)$	19 $(0,0)^-_{20}$	−0.001812	164.0	0.899	0.992
$N=20$	$^1P^0(1)$	20 $(1,1)^+_{20}$	−0.001720	157.1	0.883	0.979
	$^1P^0(2)$	20 $(3,1)^+_{20}$	−0.001691	148.6	0.812	0.913
	$^1P^0(3)$	20 $(5,1)^+_{20}$	−0.001660	142.1	0.704	0.801
	$^1P^0(4)$	20 $(0,0)^-_{21}$	−0.001642	164.5	0.891	0.992
$N=21$	$^1P^0(1)$	21 $(1,1)^+_{21}$	−0.001564	157.7	0.876	0.978
	$^1P^0(2)$	21 $(3,1)^+_{21}$	−0.001539	149.5	0.803	0.910
	$^1P^0(3)$	21 $(5,1)^+_{21}$	−0.001512	143.1	0.696	0.797
	$^1P^0(4)$	21 $(0,0)^-_{22}$	−0.001494	164.9	0.884	0.991
$N=22$	$^1P^0(1)$	22 $(1,1)^+_{22}$	−0.001428	158.3	0.868	0.977
	$^1P^0(2)$	22 $(3,1)^+_{22}$	−0.001406	150.3	0.795	0.908
	$^1P^0(3)$	22 $(5,1)^+_{22}$	−0.001383	144.0	0.687	0.793
	$^1P^0(4)$	22 $(0,0)^-_{23}$	−0.001366	165.3	0.876	0.991
$N=23$	$^1P^0(1)$	23 $(1,1)^+_{23}$	−0.001309	158.8	0.860	0.977
	$^1P^0(2)$	23 $(3,1)^+_{23}$	−0.001290	151.0	0.787	0.906
	$^1P^0(3)$	23 $(5,1)^+_{23}$	−0.001270	144.9	0.679	0.789
	$^1P^0(4)$	23 $(0,0)^-_{24}$	−0.001254	165.6	0.868	0.991
$N=24$	$^1P^0(1)$	24 $(1,1)^+_{24}$	−0.001204	159.3	0.853	0.976
	$^1P^0(2)$	24 $(3,1)^+_{24}$	−0.001188	151.7	0.779	0.904
	$^1P^0(3)$	24 $(5,1)^+_{24}$	−0.001171	145.7	0.670	0.785
	$^1P^0(4)$	24 $(0,0)^-_{25}$	−0.001155	166.0	0.861	0.990
$N=25$	$^1P^0(1)$	25 $(1,1)^+_{25}$	−0.001112	159.8	0.845	0.975
	$^1P^0(2)$	25 $(3,1)^+_{25}$	−0.001097	152.3	0.771	0.901
	$^1P^0(3)$	25 $(5,1)^+_{25}$	−0.001082	146.5	0.662	0.781
	$^1P^0(4)$	25 $(0,0)^-_{26}$	−0.001067	166.3	0.853	0.990

strong mixings and the high density of states in the spectra of DES, conjectural classifications are less revealing than what is required of theory and computation.

3 Calculations

The calculations of the present work involved two phases: in the first phase, the aim was to produce correlated wavefunctions and their energies, for a series of DES of H^- and He of $^1P^0$ symmetry, which include single as well as double virtual excitations from an intrashell multiconfigurational zero order reference space of each N manifold. In the second phase, the energies and wavefunctions of such calculations are employed for analysis of a part of the DES spectra, up to $N = 25$. Focusing on the lowest four states of each N manifold, which were obtained with very good accuracy, both the (K,T) and the (F,T) classification schemes were explored, and was found that, in fact, when electron correlation is computed well, the latter classification is the more appropriate one. These results are accompanied by results on geometrical properties.

The first report of this type of analysis was published in 1993 by Komninos *et al.* [3], where the focus was on the TEIL states, and where N went up to 15. In this work this theory is extended to the more difficult case of determining additional states above the TEIL ones beyond the low regime, by going up to $N = 25$. In what follows, we recall the basic features of the approach of [3] and explain how they relate to the present calculations.

3.1 Configurations constructed from a hydrogenic basis set

The state-specific theory of multiply states described in [1,23] and in references therein, places emphasis on the computation of a MCHF establishing localization in the continuous spectrum *via* the solution of MCHF equations, where the physically and computationally relevant configurations are included. Using this MCHF wavefunction as a reference space, the remaining part of electron correlation is added variationally. This method is numerically stable when the level of excitation is in the low regime. However, in the high regime, where the density of states and the size of their wavefunctions, especially in H^-, complicates matters considerably, a reliable solution of the appropriate MCHF equations is currently impossible. Nevertheless, the findings and conclusions reported in [3] justify the present calculations, which used hydrogenic basis sets. Specifically, natural orbitals which are obtained from basis sets of hydrogenic orbitals, when used for the construction of multiconfigurational intrashell DES produced energies which were in agreement with those obtained from a basis of self-consistent orbitals [3]. This finding, in conjunction with the earlier results of Robaux [14] who used hydrogenic basis sets and obtained meaningful results, was interpreted as attributing validity to the systematic use of hydrogenic basis sets for the calculation of diagonal matrix elements of DES of higher N.

Therefore, in the present work, the basis orbitals were hydrogenic and were computed numerically. In spite of the slow convergence which results from the inability of such orbitals to account for relaxation and screening, one advantage from their use is the fact that one can follow systematically the construction of properly symmetrized configurations, $\Phi_i(\gamma \mathrm{LS}\pi) = |n\lambda n'\lambda';\ {}^{2S+1}\mathrm{L}^\pi\rangle_i$, as well as the stability of results as the size of the set increases. For given n, n', L and π all possible values of λ and λ' can be taken into account. The $\Phi_i(\gamma \mathrm{LS}\pi)$ are used to compute the Hamiltonian matrix, whose diagonalization yields the eigenvalues E_v and eigenfunctions Ψ_v. The Ψ_v have the form:

$$\Psi_v = \sum_{n,n'=N}^{M} c_{n,n'}^{(v)} \left|n\lambda n'\lambda';\ {}^{2S+1}\mathrm{L}^\pi\right\rangle . \qquad (2)$$

Theoretical considerations and computational experience show that the hole-filling configurations representing series whose beginning is below the lowest state of the N manifold with $n, n' = 1, ..., N-1$ should be excluded from the expansion. The exclusion of all hydrogenic configurations with $n < N$ or $n' < N$ is necessary for obtaining well-converged and meaningful results.

For each N, doubly excited configurations with orbitals up to $N+3$ were also included. Specifically, all hydrogenic product functions have been included in which one of the electrons is represented by a $n\lambda$ function, $N \le n \le N+3$ and the other electron can have any radial quantum number n', $n \le n' \le N+3$. Even with the above choices, it is possible to have Ψ_v energetically degenerate with Rydberg series or with scattering continua of lower-lying hydrogen thresholds. The results of Robaux [14] as well as ours, together with conclusions from the study of the magnitude of off-diagonal matrix elements, (very small, decreasing with excitation), support the assumption that inclusion of such channels is unwarranted as regards the determination of the energies of low-lying states of each N manifold and of their geometrical properties.

The number of hydrogenic configurations used in our final calculations varied from 100 for $N = 6$ to 404 for $N = 25$. These numbers were found to produce stable results for the four lowest roots at each N manifold. Because of the CI nature of the calculation, accuracy is expected to be higher for the lowest root of the intrashell type, $(F,T) = (1,1)$, and of the intershell type, $(F,T) = (0,0)$.

3.2 Projection of the Ψ_v on the DESB

The use of group theory and of approximate quantum numbers for the labeling and description of DES, was initiated by Wulfman in 1968 [31], albeit without successful results. In 1973, Wulfman [32] and Sinanoğlu and Herrick [15,16], independently, proposed the now well-known novel schemes of approximate diagonalization of DES and of new quantum numbers which classify such states in a way that describes some effects of electron correlation. This approach was further advanced by Herrick and coworkers [20,21], producing a wealth of semiquantitative descriptions and classifications. At the core of this development, and the basis for a number of applications by Herrick and Sinanoğlu and by other researchers since then, is the DESB, which is defined in terms of hydrogenic functions and is labeled by corresponding good numbers, P and Q, as defined by Wulfman [32], or K and T, as introduced by Herrick and Sinanoğlu, [15,16,20,21]. The DESB vector is a superposition of vectors $|n\lambda n'\lambda';\ {}^{2S+1}\mathrm{L}^\pi\rangle_i$ with coefficients determined algebraically. They are given as [15,16,21]

$$\Phi_{Nn}^{(\mathrm{DESB})}\left(KT;\ {}^{2S+1}\mathrm{L}^\pi\right) = \left|NnKT\ {}^{2S+1}\mathrm{L}^\pi\right\rangle = \sum_{\lambda_1\lambda_2} D_{N\lambda_1 n\lambda_2}^{KTL\pi} \left|N\lambda_1 n\lambda_2;\ {}^{2S+1}\mathrm{L}^\pi\right\rangle \qquad (3)$$

where $D_{N\lambda_1 n\lambda_2}^{KTL\pi}$ is proportional to a 9-j vector coupling coefficient.

The numbers (K,T) are used to label DES. States having the same N, K and T form a Rydberg series. Although n is not a good number, in general, it corresponds to the highest component $D_{N\lambda_1 n\lambda_2}^{KTL\pi}$ for the lowest states of the series. For each value of L, T is restricted to the integers 0, 1, ..., $\min(L, N-1)$ and $\mu K = N-T-1$, $N-T-3$, ..., 1 or 0. Moreover if $\pi = (-1)^{L+1}$, then $T > 0$. K is proportional to $\langle r_< \cos\theta_{12}\rangle$, where $r_<$ refers to the inner electron. For different series, $\cos\theta_{12}$ is in general negative if $K > 0$, and positive if $K < 0$. Hence, a positive value of K is taken to correspond to the electrons being on opposite sides of the ionic core, thereby decreasing repulsive interaction. On the other hand, a negative value of K corresponds to electrons being on the same side of the core.

In this case, repulsion is stronger and the energies of these states is higher.

The evaluation of the exactness of the approximate quantum numbers K and T is done by projecting the variationally calculated wavefunctions Ψ_v of equation (2) onto the DESB function of equation (3):

$$\left\langle \Psi_v \middle| \Phi_{nn'}^{(\mathrm{DESB})}(KT) \right\rangle = \sum c_{nn'}^{(v)} D_{nln'l'}^{KT} = \alpha_v(nn' : KT). \tag{4}$$

The sum:

$$P_v(KT) = \sum_{n,n'} \left[\alpha_v(nn' : KT)\right]^2 \tag{5}$$

gives the fraction of the contribution to Ψ_v of DESB functions with common K and T. The characterization of a DES by individual K and T numbers is done by selecting the largest scalar product in the sum of equation (5).

For the DES of $^1\mathrm{P}^0$ symmetry, $T = 1$ for the intrashell DESB states ($N = n$), and $T = 0$ or 1 for the intershell DESB states ($N \neq n$). Therefore, the $^1\mathrm{P}^0$ DES offer the opportunity of testing whether T is a good number. The numerical results of [3] showed that for the TEIL DES up to $N = 15$, T is a good number. However, the N and the K are not good numbers even for the TEIL states, losing accuracy as excitation energy increases and Coulomb attraction decreases.

3.3 The FT classification scheme

The degree of the goodness of the DESB wavefunctions for low-lying DES, *i.e.* of the $|K, T, N, n; L, S, \pi\rangle$ representation, was studied by Lin and Macek [28], by comparing them to configuration-interaction (CI) wavefunctions which had been computed by Lipsky, Anania and Conneely [33] using hydrogenic basis sets. They concluded that the DESB approximation "*emphasizes angular correlations and underrepresents radial correlation*" (p. 2317 of [28]), and that "*for some series they give accurate representations but not for others*" (p. 2321 of [28]).

Komninos *et al.* [3] recognized that even in the case of the well-correlated TEIL states, the (K, T) eventually breaks down as N increases, and that the cause of this breakdown is the neglect of the double excitations which is intrinsic to the model. They also reported the results of preliminary calculations, which have now been extended and completed, according to which: "*For the other intrashell states of each N-manifold, matters deteriorate for lower values of N*" (p. 405 of [3]). As a remedy to this fact, Komninos *et al.* [3] proposed that instead of K, a combination of K and N should be used, where now, neither K nor N are good numbers. (T remains a "good" number.) Indeed, the choice of F, given by equation (1), in conjunction with well-correlated wavefunctions, has shown that the F, T scheme does better.

F depends on N and K but we do not relate this number to DESB functions directly. The range of F is

$$T \leq F \leq 2N - 2 - T, \text{ in steps of 2.} \tag{6}$$

In this representation, the wavefunction of a DES is written as

$$\Psi_{Nn}\left(^{2S+1}\mathrm{L}^{\pi}\right) \approx \sum_{n_1 n_2} c_{n_1 n_2} \Phi_{n_1 n_2}\left(FT;\ ^{2S+1}\mathrm{L}^{\pi}\right) \tag{7}$$

where $N \leq n_1 \leq n_2$. This formal expansion is by construction more accurate, since it includes single and double excitations from a single DESB function. Perturbation theory shows that using wavefunctions containing only single excitations cannot be reliable, especially for excited states where strong mixings is the rule.

It is important to note that whereas the DESB vectors are the same for all Z, the FT ones are not. The quality of the (F, T) classification scheme depends on the system and on the level of excitation and can be investigated by numerical calculations.

The projection of the wavefunction Ψ_v onto the FT vectors is done formally by a summation of the squared coefficient $\alpha_v(nn' : KT)$ for all triplets of n, n' and K, which give a common value for the quantum number F:

$$P_v(FT) = \sum_{k,n,n'} \left[\alpha_v(nn' : (K = N - F - 1)T)\right]^2. \tag{8}$$

The evaluation of the degree of goodness of T is done simply by selecting the individual contributions of all allowed values. This procedure is applied for all values of K or F.

In classifying our results, we have also used the Herrick-Lin number A [9,21], defined by

$$A = \begin{cases} \pi(-1)^{S+T} & \text{if } K > L - N \\ 0 & \text{if } K \leq L - N \end{cases}. \tag{9}$$

A is not independent of K and T and can take the value $+1$ (-1) or 0, depending on the presence or absence of a node (antinode) at $r_1 = r_2$. For intrashell states A is always unity. We will follow, as do other workers, the notation ${}_N(K, T)_n^A$ for a state in a series, with the quantum number n of the outer electron starting from N or $N + 1$, depending on the series.

3.4 Mean values and geometry

The possibility of a better understanding of DES is connected to the possibility of acquiring quantitative information about the correlated motion of the electrons. Main characteristics of this motion are revealed by probability densities and average values. In this regard, the calculation of the correlated $\langle r_1 \rangle$ and $\langle r_2 \rangle$ under the assumption that the two electrons occupy approximately the same region, is done by using the expressions [1]

$$\langle r_1 \rangle = \iiint \rho\left(r_1, r_2, \cos\theta_{12}\right) r_1 \sin\theta_{12} \mathrm{d}r_1 \mathrm{d}r_2 \mathrm{d}\theta_{12} \tag{10a}$$

$$\langle r_2 \rangle \,|_{r_1 = \langle r_1 \rangle} = \frac{\iint \rho\left(\langle r_1 \rangle, r_2, \cos\theta_{12}\right) r_2 \sin\theta_{12} \mathrm{d}r_2 \mathrm{d}\theta_{12}}{\iint \rho\left(\langle r_1 \rangle, r_2, \cos\theta_{12}\right) \sin\theta_{12} \mathrm{d}r_2 \mathrm{d}\theta_{12}}. \tag{10b}$$

$\rho(r_1, r_2, \cos\theta_{12})$ is the exact electron density of the state of interest and $\rho(\langle r_1\rangle, r_2, \cos\theta_{12})$ is the density that results if r_1 is fixed at the average value $\langle r_1\rangle$ and the angular dependence on θ_{12} is integrated.

We have also computed $\langle\cos\theta_{12}\rangle$, and have compared the results to those obtained from the application of the DESB formula for intrashell states [21]

$$\langle\cos\theta_{12}\rangle_{\mathrm{DESB}} = \frac{4N^2 - 3(N+K)^2 - 3T^2 + 2L(L+1) - 1}{8N^2}. \tag{11}$$

For the *ab initio* calculation with the correlated wavefunctions, we used

$$\langle\cos\theta_{12}\rangle = \iiint \rho\,(r_1, r_2, \cos\theta_{12})\cos\theta_{12}\sin\theta_{12}\mathrm{d}r_1\mathrm{d}r_2\mathrm{d}\theta_{12}. \tag{12}$$

The problem of the calculation of the interelectronic angle θ_{12} in the general case of polyelectronic atomic states was solved by Komninos and Nicolaides [23] by proving a connection to R^k integrals obtained from the electronic structure of the state. The present case is simple, and so $\rho(\cos\theta_{12})$ can be calculated straightforwardly. The mean value $\langle\theta_{12}\rangle$ is calculated as $\langle\theta_{12}\rangle = \cos^{-1}\langle\cos\theta_{12}\rangle$.

4 Results

Our results are given in Tables 1–6 and in Figures 1–6. The information which is contained in them pertains to energies, to classification based on the schemes of (K,T) and (F,T) and to geometries based on the averages of the angle θ_{12} and of the radii.

4.1 Energies

Tables 1 and 2 contain, together with other essential results of our calculations, the energies for He and for H^-. For each manifold up to $N = 25$ we obtained data for the lowest four states of $^1P^0$ symmetry, which are labeled by the F,T numbers, in addition to N, n, and A. The number four was deemed sufficient to deduce useful conclusions, apart from the value of knowing the positions of a large number of hitherto unknown DES that are in principle reachable *via* photoabsorption of the ^1S ground state.

We already stated in Section 3.1 the method of calculation and of inclusion of virtual configurations. At the end of the section, in Section 4.4, we present the results of a typical convergence study, using the $N = 23$ $^1P^0$ lowest DES of H^-. (Convergence for neutral and positive ion DES is always easier.)

The positions of the TEIL states are presented in Figure 1 (He) and Figure 2 (H^-) together with positions of the hydrogenic levels. As excitation increases, more and more hydrogen thresholds come below the energies of the TEIL states. If widths were to be computed by an all-orders theory, this fact implies the addition of considerable complexity before an understanding toward the accurate calculation of widths of DES in the regime of high excitation can be. In this respect, we cite the work of Bylicki and Nicolaides [34] on the resolution of the resonance spectra of H^- below the $n = 5$ hydrogenic threshold, for an evaluation of the demands that such calculations would have when the high regime region is examined.

The validity of the calculations as regards the accuracy of the energies, apart from the internal consistency and convergence tests that were applied, is confirmed by the favorable comparison with results of other advanced methods which are available for the regime of low excitation, up to $N = 13$ (Tabs. 3 and 4). It is this type of accuracy that characterizes all the energies computed in this work, for 80 states for H^- and for He up to $N = 25$. We point out that even for the low regime a large number of new energy levels are presented here.

As regards the He spectrum, when $N = 6$–9 the fourth root represents an intershell state, with the assignment of $F = 0$ and $T = 0$. Geometrical characteristics of this state, as well as those of other states, are analyzed in the following subsections. Starting at $N = 10$ up to $N = 25$, the lowest four roots represent intrashell states with $T = 1$. On the other hand, in H^- the $(0,0)$ intershell state starts from the second position for $N = 6$, stays in the third position for $N = 7$ to $N = 14$, and moves to the fourth position for $N = 15$ up to 25. This is in harmony with a general behavior of low-lying spectra in polyelectronic atoms: as Z decreases and the relative importance of interelectronic repulsion and correlation increases, Rydberg states come below valence states. In the present cases, the observed behavior is a manifestation of the changes in screening, (less when excitation of both electrons is high), and of the relative strengths of the contribution of the three parts of the energy operator (kinetic energy, nuclear attraction and electron repulsion).

4.2 Classification

In Tables 1 and 2, the effectiveness of the (K,T) and (F,T) schemes in providing high purity states is compared. It is clear that the (F,T) scheme expresses the character of the DES better, in both the intrashell, $T = 1$, and the intershell, $T = 0$, cases. In fact, for the TEIL states, the (F,T) representation remains rather good even up to $N = 25$, whereas the (K,T) one deteriorates significantly. These facts are depicted in a clear way with the example of Figure 3, where we have plotted the purity coefficients of the lowest intrashell DES, $(F,T) = (1,1)$, (the TEIL state), and of the lowest intershell DES, $(F,T) = (0,0)$ of H^-, as a function of N.

In Tables 5 and 6, the content of (F,T) character for the states $N = 6$, 10, 15, 20 and 25 is presented. Due to symmetry, for intershell states T can have two values, $T = 0$ and 1. Therefore, they offer the opportunity of testing the goodness of T, since some of the states in our calculation exhibit intershell character (see the subsection on geometry below). Our calculations show that T is

Table 3. Comparison of the present results for the energies of some H^- low-lying DES with available results from the literature.

State		(a)	(b)	(c)	(d)	(e)	(f)	(g)
$N = 6$	$^1P^0(1)$	−0.017560	−0.017434	−0.01752	−0.0170	−0.017375	−0.01739	−0.017333
	$^1P^0(2)$	−0.016150		—		—	−0.01609	—
	$^1P^0(3)$	−0.016037		—		−0.01589	−0.01564	—
	$^1P^0(4)$	−0.015307		−0.01537			−0.015255	−0.01525
$N = 7$	$^1P^0(1)$	−0.013109	−0.013017	−0.01298	−0.0127	−0.01293	−0.01299	−0.012877
	$^1P^0(2)$	−0.012202		—		−0.012025	—	—
	$^1P^0(3)$	−0.012103		—			−0.01206	—
	$^1P^0(4)$	−0.011530		−0.01156			−0.01152	−0.011289
$N = 8$	$^1P^0(1)$	−0.010158	−0.010086	−0.01009	−0.00990			−0.010017
	$^1P^0(2)$	−0.009578		—				—
	$^1P^0(3)$	−0.009417		—				—
	$^1P^0(4)$	−0.009013		−0.00905				−0.008803
$N = 9$	$^1P^0(1)$	−0.008103	−0.008045	−0.00802	−0.00791			
$N = 10$	$^1P^0(1)$	−0.006615		−0.00653	−0.00647			
$N = 11$	$^1P^0(1)$	−0.005503		−0.00542	−0.00539			
$N = 12$	$^1P^0(1)$	−0.004650		−0.00456	−0.00455			
$N = 13$	$^1P^0(1)$	−0.003981			−0.00390			

(a) This work, (b) Nicolaides and Komninos, reference [2], (c) Sadeghpour and Greene, reference [8], (d) Rost and Briggs, reference [10], (e) Ho, reference [29], (f) Koyama, Takafuji and Matsuzawa, reference [7], (g) Harris *et al.*, reference [36], experiment.

Table 4. As in Table 3, for He.

State		(a)	(b)	(c)	(d)	(e)	(f)	(g)
$N = 6$	$^1P^0(1)$	−0.089021	−0.088984	−0.08924	−0.0867	−0.0886	−0.08888	−0.088603
	$^1P^0(2)$	−0.085019		−0.08330			—	−0.084825
	$^1P^0(3)$	−0.079875					—	−0.079999
	$^1P^0(4)$	−0.079599					−0.0795	−0.079516
$N = 7$	$^1P^0(1)$	−0.065903	−0.065871	−0.06612	−0.0644		−0.06645	−0.065509
	$^1P^0(2)$	−0.063569		−0.06243			—	−0.063276
	$^1P^0(3)$	−0.060682					—	−0.060473
	$^1P^0(4)$	−0.059602					−0.05975	−0.059511
$N = 8$	$^1P^0(1)$	−0.050743	−0.050714	−0.05113	−0.0498			
	$^1P^0(2)$	−0.049271		−0.04842				
$N = 9$	$^1P^0(1)$	−0.040271	−0.040247	−0.04040	−0.0396			
	$^1P^0(2)$	−0.039286		−0.03888				
$N = 10$	$^1P^0(1)$	−0.032737	−0.032718	−0.03289	−0.0323			
$N = 11$	$^1P^0(1)$	−0.027136			−0.0268			
$N = 12$	$^1P^0(1)$	−0.022860			−0.0226			
$N = 13$	$^1P^0(1)$	−0.019522			−0.0193			

(a) This work, (b) Komninos and Nicolaides, reference [2], (c) Sadeghpour, reference [8], (d) Rost and Briggs, reference [10], (e) Ho, reference [37], (f) Koyama, Takafuji and Matsuzawa, reference [7], (g) Rost, Schultz, Domcke and Kaindl, reference [38].

Table 5. FT character of H^- DES states of $^1P^0$ symmetry at selected N manifolds up to $N = 25$. F, T remain good as N increases not only for the TEIL state but also for the lowest intershell state $(0, 0)$. Note that the $(0, 0)$ state is the second root at $N = 6$ and the fourth one at $N = 25$. Compared to He, in H^- the (F, T) scheme loses accuracy faster as N increases. States marked by (•) have a small contribution from other FT vectors not shown here.

		(F,T)							
		$(1,1)$	$(3,1)$	$(5,1)$	$(7,1)$	$(0,0)$	$(2,0)$	$(4,0)$	$(6,0)$
$N=6$	$^1P^0(1)$	98.76	1.20	0.02			0.02		
	$^1P^0(2)$	0.02				99.64	0.34		
	$^1P^0(3)$	1.21	93.33	5.18	0.19			0.06	0.01
	$^1P^0(4)$	98.61	1.09	0.03		0.01	0.24		
$N=10$	$^1P^0(1)$	98.62	1.36	0.02					
	$^1P^0(2)$	1.24	93.68	4.91	0.15			0.01	
	$^1P^0(3)$					99.52	0.47		
	$^1P^0(4)$ •	0.05	4.71	83.37	11.08			0.02	
$N=15$	$^1P^0(1)$	98.23	1.74	0.03					
	$^1P^0(2)$	1.66	92.52	5.62	0.19				
	$^1P^0(3)$ •	0.03	5.40	82.18	11.63				
	$^1P^0(4)$					99.34	0.65		
$N=20$	$^1P^0(1)$	97.86	2.10	0.04					
	$^1P^0(2)$	2.05	91.26	6.45	0.24				
	$^1P^0(3)$ •	0.04	6.28	80.08	12.71				
	$^1P^0(4)$					99.16	0.83		
$N=25$	$^1P^0(1)$	97.54	2.41	0.05					
	$^1P^0(2)$	2.37	90.15	7.18	0.29				
	$^1P^0(3)$ •	0.05	7.05	78.10	13.76				
	$^1P^0(4)$					99.01	0.98	0.01	

Table 6. As in Table 5, for He. F deteriorates slowly from the lowest to the fourth intrashell ($T = 1$) state, especially for high N, where radial correlation acquires relatively more importance. The TEIL state (lowest energy) keeps a rather good FT character all the way up to $N = 25$.

		(F,T)							
		$(1,1)$	$(3,1)$	$(5,1)$	$(7,1)$	$(0,0)$	$(2,0)$	$(4,0)$	$(6,0)$
$N=6$	$^1P^0(1)$	99.72	0.26						
	$^1P^0(2)$	0.04	98.33	1.56	0.02		0.01	0.03	
	$^1P^0(3)$ •	0.01	0.89	92.83	5.85			0.01	0.14
	$^1P^0(4)$	0.03				99.90	0.07		
$N=10$	$^1P^0(1)$	99.76	0.23						
	$^1P^0(2)$	0.10	98.72	1.15	0.01				
	$^1P^0(3)$ •		0.73	95.63	3.55				0.02
	$^1P^0(4)$ •		0.01	2.65	88.53				
$N=15$	$^1P^0(1)$	99.62	0.38						
	$^1P^0(2)$	0.30	98.18	1.51	0.02				
	$^1P^0(3)$ •		1.25	94.85	3.81				
	$^1P^0(4)$ •		0.01	3.26	88.70				
$N=20$	$^1P^0(1)$	99.39	0.60						
	$^1P^0(2)$	0.54	97.31	2.12	0.03				
	$^1P^0(3)$ •		1.94	93.12	4.82				
	$^1P^0(4)$ •		0.03	4.44	86.29				
$N=25$	$^1P^0(1)$	99.14	0.85	0.01					
	$^1P^0(2)$	0.81	96.35	2.80	0.05				
	$^1P^0(3)$ •		2.66	91.17	5.98				
	$^1P^0(4)$ •		0.05	5.70	83.31				

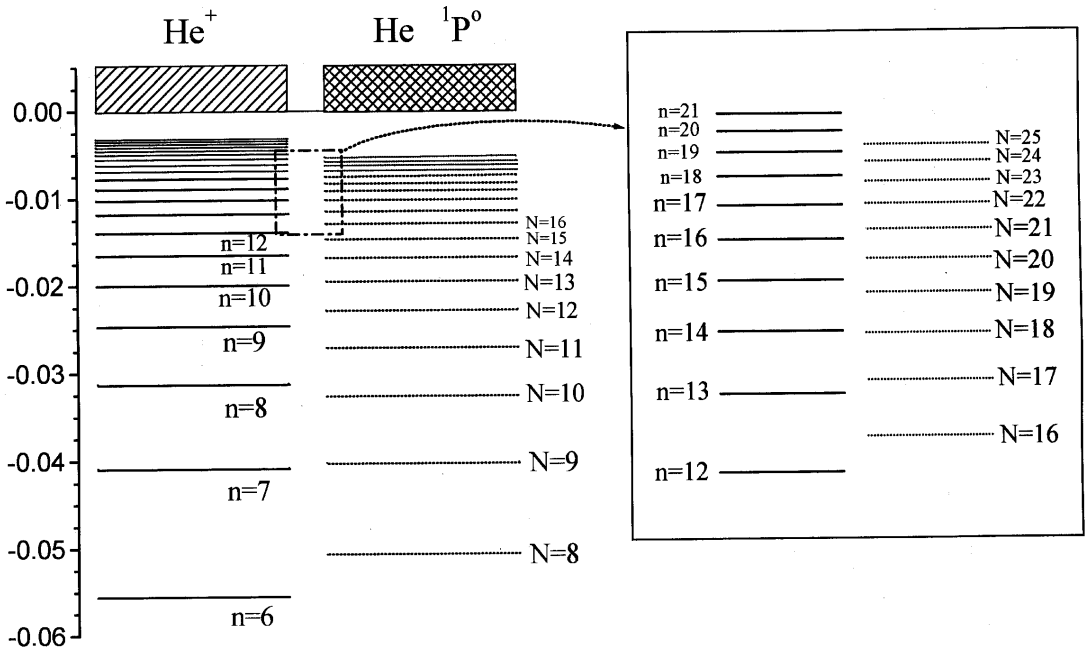

Fig. 1. Comparison of the energies of the He TEIL states with the hydrogenic thresholds. The crossing of a lower hydrogenic threshold starts with $N = 5$, which is below the $n = 4$ He^+ threshold (not shown here). As (N, n) increase, the TEIL state for each N is found below many hydrogenic thresholds.

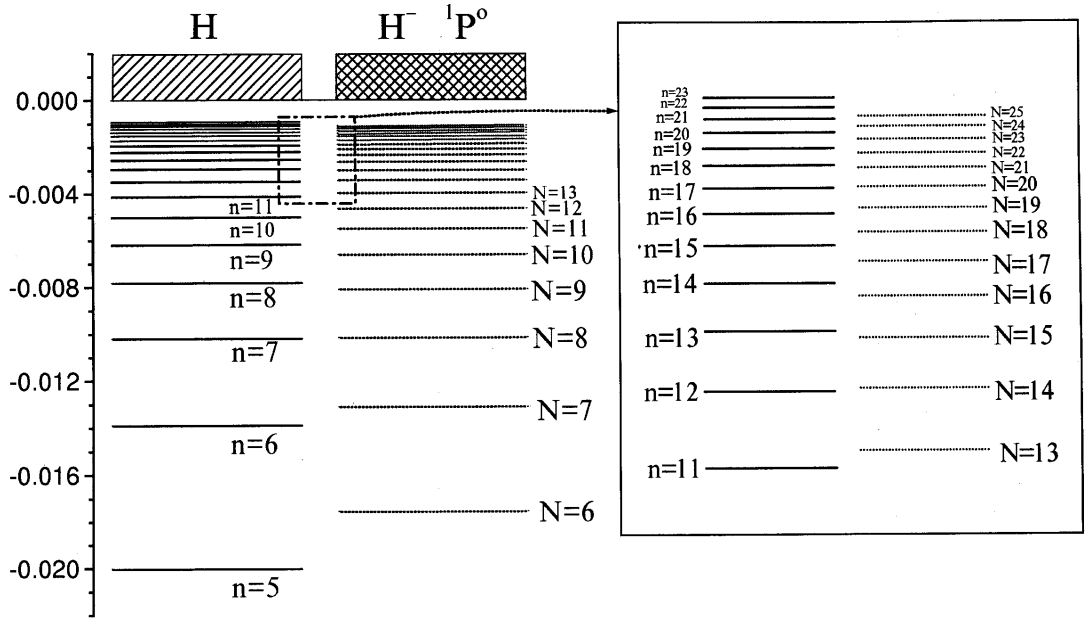

Fig. 2. Same comparison as in Figure 1, for the H^- states.

a good number for all the studied states. Mixing of configurations having different values of T is negligible.

Tables 5 and 6 show that mixing of the various (F, T) vectors is very small. Each $^1P^0$ state is characterized by a specific (F, T) combination. Not only the TEIL state, which is the lowest intrashell state, but also the lowest intershell state, which is labeled by $(0, 0)$, keep high purity for all N. In general, the (F, T) label is less accurate in H^- than in He, as N increases.

4.3 Geometry

The geometrical features of the (F, T) states were obtained from the expectation values of the angle θ_{12} and of the radii. These are presented in Figures 4–6 for $\langle\theta_{12}\rangle$ and in Figure 7 for the radii. The numerical values of $\langle\theta_{12}\rangle$ are given in Tables 1 and 2. In addition, the results obtained for the DESB states, which are Z-independent, are plotted in the figures. For the intrashell states, Herrick's

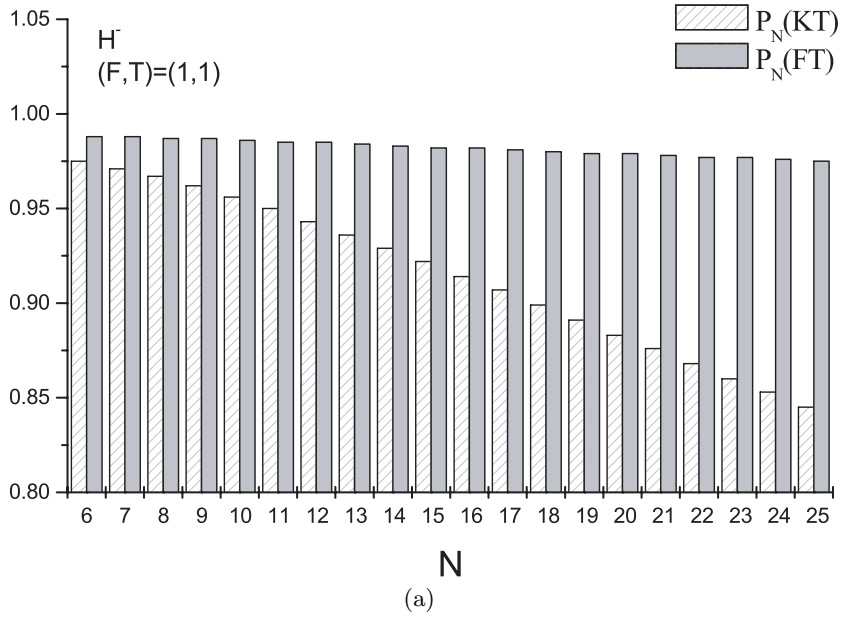

(a)

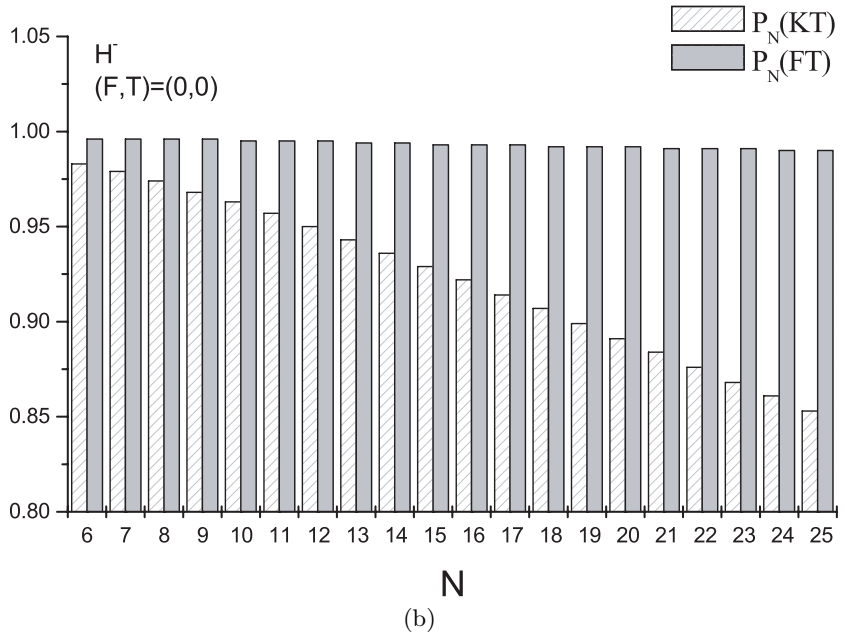

(b)

Fig. 3. (K,T) and (F,T) purity coefficient for the lowest $^1\mathrm{P}^0$ intrashell DES, $(F,T)=(1,1)$ and for the lowest $^1\mathrm{P}^0$ intershell DES, $(F,T)=(0,0)$ of H^-, as a function of the hydrogenic manifold number N. Their calculation was done in terms of the CI wavefunctions described in the paper, and equations (5, 8).

formula (11) was used. For the $(F,T)=(0,0)$ state, which is of the intershell $(N,N+1)$ type, the formula for the average of the angle was obtained as

$$\langle\cos\theta_{12}\rangle_{\mathrm{DESB}}=\frac{-4N^3+6N^2-2}{(N+1)(2N-1)^2}\cdot \qquad (13)$$

Formula (13) was derived from the formula (A15) of de Prunelé [35] for $L=1$, which is applicable to the case of $T=0$.

The results for $\langle\theta_{12}\rangle$ are consistent, systematic and revealing. The lowest state, $(1,1)$, which is the TEIL state, has the largest angle of the intrashell states. This reflects the fact that as electron correlation is reduced for the higher-lying states, the interelectronic angle is reduced as well. The *ab initio* angle is a bound from above to the DESB result and tends to 180° as N goes to infinity. If this feature is combined with findings for the average radii of Figure 6, which shows that $\langle r_1\rangle\sim\langle r_2\rangle|_{r_1=\langle r_1\rangle}$ is satisfied not only for the TEIL state but for the other two intrashell states as well, we obtain a good picture of the trends in the geometry of such DES.

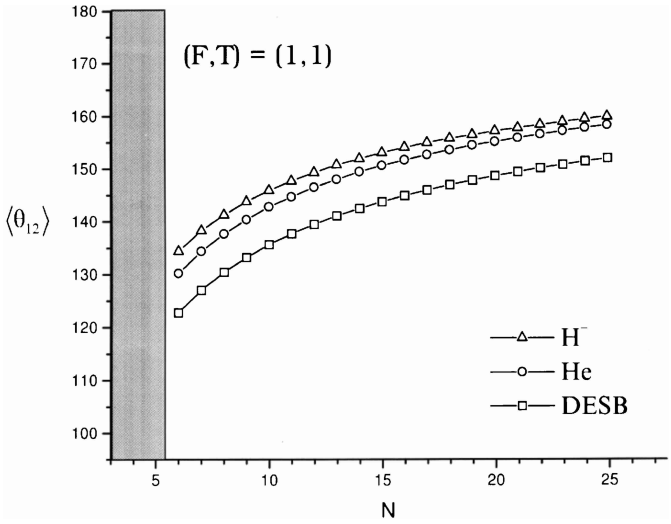

Fig. 4. Mean value $\langle\theta_{12}\rangle$ of the interelectronic angle of $^1P^0$ resonances of He and H^-, having $(F,T) = (1,1)$. DESB values are calculated by the formula (11). For TEIL states, electron correlation is more important in H^-. Therefore, already at low N, the angle is larger than that of He and of the DESB state. All tend to $\langle\theta_{12}\rangle = 180°$.

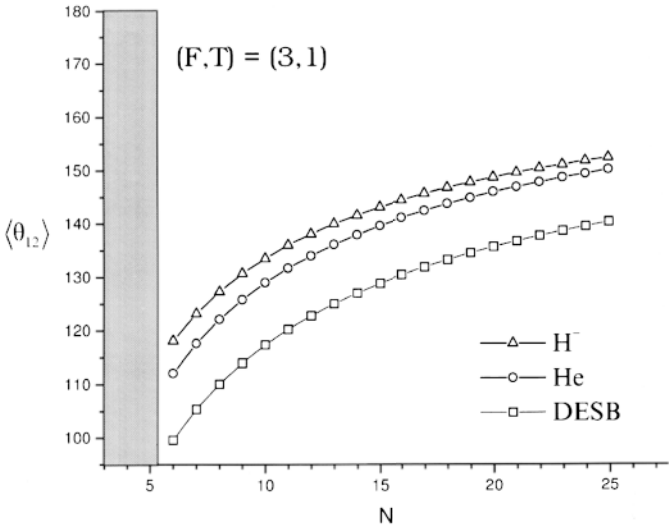

Fig. 5. Same as Figure 3 for the states with $(F,T) = (3,1)$. The second intrashell state starts from smaller values than the Wannier TEIL ones and remain so up to $N = 25$.

On the other hand, the state $(0,0)$ exhibits the intershell character in Figure 6, and has a higher value than that of the intrashell states for the angle along the whole ladder of N.

Note that in all cases, the DESB results underestimate the opening of the angle, especially in H^- where electron correlation is more important.

4.4 Convergence

Finally, in Table 7 we present a typical set of results concerning convergence as a function of inclusion of singly

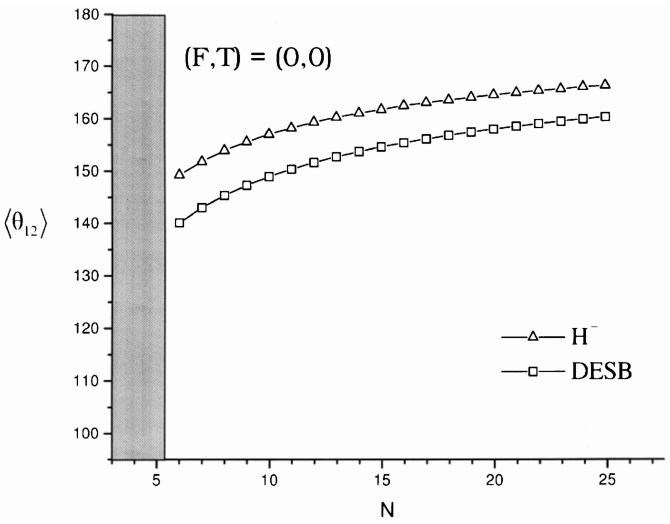

Fig. 6. Mean value $\langle\theta_{12}\rangle$ of the interelectronic angle of the lowest $^1P^0$ intershell state of H^-, having $(F,T) = (0,0)$. The intershell DESB calculation was done from formula (13).

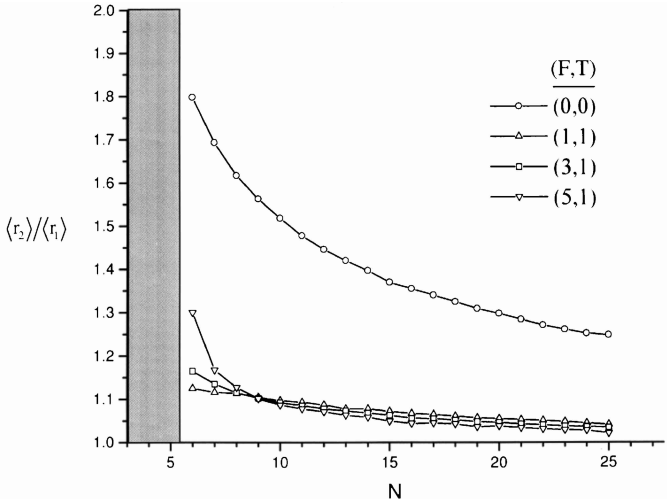

Fig. 7. Ratio of the mean values $\langle r_1\rangle$ and $\langle r_2\rangle|_{r_1=\langle r_1\rangle}$ of the lowest four $^1P^0$ resonances of H^-, at each threshold. The intrashell and the intershell character of states having $T = 1$ and $T = 0$ respectively, is clear.

and doubly excited configurations with n higher than the reference manifold. The example is taken from the calculation on the $N = 23$ states of H^-. Convergence for the lowest tree roots is well achieved when n exceeds N by two. For the fourth state the accuracy is slightly less.

5 Conclusion

A critical reading of the theories and their results which have been published during the past few decades on the subject of DES should reveal to the interested reader that an open and challenging issue has been the possibility of applying quantum mechanics to the calculation of highly excited such states. In the work reported in this paper

Table 7. Convergence of the energy of the four lowest states of the manifold $N = 23$ of H^-, as the number of singly and doubly excited hydrogenic configurations increases, with n' higher than N (see Eq. (2)).

$N(F,T)_n^A \diagdown n'$	23	24	25	26	27
23 $(1,1)_{23}^+$	−0.001169	−0.001306	−0.001309	−0.001309	−0.001309
23 $(3,1)_{23}^+$	−0.001132	−0.001286	−0.001290	−0.001290	−0.001290
23 $(5,1)_{23}^+$	−0.001090	−0.001265	−0.001270	−0.001270	−0.001270
23 $(0,0)_{24}^-$	−0.001045	−0.001243	−0.001249	−0.001254	−0.001254

on the properties of $^1P^0$ DES in He and in H^- up to $N = 25$, we demonstrated that practical calculations of well-correlated wavefunctions are possible in the regime of high N, defined here as $N > 15$. The calculations revealed a wealth of new data, for 80 $^1P^0$ DES of H^- and 80 $^1P^0$ DES of He, whose systematic analysis led to reliable conclusions regarding classification schemes, energies and geometries.

The predictions of energies are verifiable, in principle, *via* high resolution measurements of photoabsorption from the ^1S ground state.

An examination of the validity of the (K,T) classification scheme was carried out, as a function of excitation, for the lowest four localized solutions of each manifold N. Given that the correlated wavefunctions include single as well as double virtual excitations from the intrashell zero order reference space of each N, it was established that K loses accuracy as N increases. Instead, a more general number, F, whose numerical value is $N - K - 1$, where N and K are not "good" numbers, represents each state more faithfully. Since F is numerically equal to the Herrick "rovibrational" quantum number v, also appears in the approximate molecular orbital model of [10], our results on the goodness of the (F,T) scheme provide a quantitative justification of the decoupling assumptions particular to this model.

Similar calculations are possible for higher excitations as well as for other symmetries. As regards the latter, of interest would be the evaluation of the degree of validity of the (F,T) scheme in DES with $L = D$, F etc.

SIT would like to thank the Greek Scholarships Foundation (IKY) for financial support.

References

1. Y. Komninos, C.A. Nicolaides, J. Phys. B **19**, 1701 (1986); Y. Komninos, M. Chrysos, C.A. Nicolaides, J. Phys. B **20**, L791 (1987).
2. C.A. Nicolaides, Y. Komninos, Phys. Rev. A **35**, 999 (1987).
3. Y. Komninos, S.I. Themelis, M. Chrysos, C.A. Nicolaides, Int. J. Quant. Chem. Symp. **27**, 399 (1993).
4. S.I. Themelis, C.A. Nicolaides, J. Phys. B **28**, L379 (1995).
5. U. Fano, Rep. Prog. Phys. **46**, 97 (1983).
6. H.Y. Wong, A.R.P. Rau, Phys. Rev. A **38**, 4446 (1988); L. Zhang, A.R.P. Rau, Phys. Rev. A **46**, 6933 (1992).
7. N. Koyama, A. Takafuji, M. Matsuzawa, J. Phys. B **22**, 553 (1989); J.-Z. Tang, S. Watanabe, M. Matsuzawa, C.D. Lin, Phys. Rev. Lett. **69**, 1633 (1992).
8. H.R. Sadeghpour, C.H. Greene, Phys. Rev. Lett. **65**, 313 (1990); H.R. Sadeghpour, Phys. Rev. A **43**, 5821 (1991).
9. C.D. Lin, Phys. Scripta T **46**, 65 (1993).
10. J.M. Feagin, J.S. Briggs, Phys. Rev. A **37**, 4599 (1988); J.M. Rost, J.S. Briggs, J. Phys. B **24**, 4293 (1991); A. Vollweiter, J.M. Rost, J.S. Briggs, J. Phys. B **24**, L 155 (1991).
11. K. Richter, D. Wintgen, J. Phys. B **23** L197 (1990); G. Tanner, D. Wintgen, Phys. Rev. Lett. **75**, 2928 (1995).
12. P.V. Grujic, N.S. Simonovic, J. Phys. B **28**, 1159 (1995).
13. B. Gremaud, P. Gaspard, J. Phys. B **31**, 1671 (1998).
14. O. Robaux, J. Phys. B **20**, 2347 (1987).
15. O. Sinanoğlu, D.R. Herrick, J. Chem. Phys. **62**, 886 (1975).
16. D.R. Herrick, O. Sinanoğlu, Phys. Rev. A **11**, 97 (1975).
17. A.R.P. Rau, J. Phys. B **16**, L699 (1983).
18. S.J. Buckman, P. Hammond, F.H. Read, G.C. King, J. Phys. B **16**, 4039 (1983); S.J. Buckman, D.S. Newman, J. Phys. B **20**, L711 (1987).
19. M. Bylicki, J. Phys. B **30**, 189 (1997).
20. D.R. Herrick, M.E. Kellman, Phys. Rev. A **21**, 418 (1980); D.R. Herrick, M.E. Kellman, R.D. Polliak, Phys. Rev. A **22**, 1517 (1980).
21. D.R. Herrick, Adv. Chem. Phys. **52**, 1 (1983).
22. C.A. Nicolaides, M. Chrysos, Y. Komninos, Phys. Rev. A **41**, 5244 (1990).
23. Y. Komninos, C.A. Nicolaides, Phys. Rev. A **50**, 3782 (1994).
24. C.A. Nicolaides, M. Chrysos, Y. Komninos, Phys. Rev. A **39**, 1523 (1989).
25. C.A. Nicolaides, Y. Komninos, J. Phys. B **23**, L571 (1990).
26. T.A. Heim, A.R.P. Rau, J. Phys. B **28**, 5309 (1995).
27. G.S. Ezra, R.S. Berry, Phys. Rev. Lett. **52**, 1252 (1984); C.D. Lin, Phys. Rev. Lett. **52**, 1253 (1984); A.R.P. Rau, in *Atomic Physics*, edited by R.S. van Dyck, E.N. Fortson (World Scientific, Singapore, 1984), Vol. 9, p. 491.
28. C.D. Lin, J.H. Macek, Phys. Rev. A **29**, 2317 (1984).
29. Y.K. Ho, Phys. Rev. A **41**, 1492 (1990).
30. A.K. Bhatia, Y.K. Ho, Phys. Rev. A **50**, 4886 (1994).
31. C.E. Wulfman, Phys. Lett. A **26**, 397 (1968).
32. C.E. Wulfman, Chem. Phys. Lett. **23**, 370 (1973); C.E. Wulfman, Chem. Phys. Lett. **40**, 139 (1976).
33. L. Lipsky, R. Anania, M.J. Conneely, At. Data Nucl. Data Tables **20**, 127 (1977).
34. M. Bylicki, C.A. Nicolaides, Phys. Rev. A **61**, 052508 (2000).
35. E. de Prunelé, Phys. Rev. A **44**, 90 (1991).
36. P.J. Harris *et al.*, Phys. Rev. Lett. **65**, 309 (1990).
37. Y.K. Ho, J. Phys. B **15**, L691 (1982).
38. J.M. Rost, K. Schultz, M. Domcke, G. Kaindl, J. Phys. B **30**, 4663 (1997).